

HEAT TRANSFER BEHAVIOR OF A PTC RECEIVER TUBE USING TRANSVERSAL FOCAL INSERTS AND CFD

HADDOUCHE M.R.*, HADDOUCHE A.**

*Department of Computer and Industrial Engineering, university of Lleida, 25001, Catalonia, Spain.

**Department of Mechanical Engineering, university of Abou Bekr-Belkaid, 13000, Tlemcen, Algeria

haddouchemedred@outlook.es

Abstract - The thermohydraulic performance of an enhanced PTC's tube is evaluated in this paper. A passive method is used by introducing transversal inserts on the bottom part of the receiver. The height of the inserts is investigated using MCRT method coupling FVM for Reynolds number range from $2.36 \cdot 10^4$ to $11.83 \cdot 10^4$. The heat transfer fluid used in this study is the Therminol®VP1. The numerical results show that the tube enhanced by inserts augments the reliability of the system, and the introduction of the inserts into the receiver tube decreases the temperature difference over the circumferential area of the absorber tube and minimizes the heat losses and also increase the lifetime of the receiver.

Keywords: Parabolic trough solar collector, inserts, thermal performance, Computational Fluid Dynamic, nonuniform heat flux.

1. INTRODUCTION

One of the cleaners, renewable, cost-free, and available sources of energy on earth is solar energy. The earth receives the incident solar radiation at a rate of approximately $8 \cdot 10^{16}$ W, more than 10.000 times the world energy consumption [1]. With the aim to be useful, this energy should be collected. There are two main groups of solar concentrators: Punctual, like solar tower and parabolic dish, and linear, like linear Fresnel collector and Parabolic Trough Collector (PTC) [2]. In order to achieve a good efficiency, a high technology is needed.

Parabolic Through Collectors are considered the desired systems with low-cost technology and simple structures for heat applications higher than 400 °C [3, 4]. The PTC technology is mainly consisted of a long parabolic shaped mirror and an absorber tube. The key element of this system is the receiver where the sun rays are concentrated and transformed to useful energy [5]. The receiver tube is covered by a glass casing in order to minimize heat losses to the environment by maintaining a vacuum in the annular space.

Moreover, a lot of investigators and engineers focused on the thermal behavior of the HTF inside the absorber tube and also decrease its temperature gradient by different methods, and also reduce the heat losses to the ambient. Gong et al. [6] analyzed numerically the heat transfer

enhancement of a PTC's absorber tube by using fins type inserts with the objective to improve the thermal behavior of the HTF inside the tube and decrease the tube circumferential temperature gradient. Their results show that both *Nu* number and the receiver's thermal performance were augmented after the PFAI-PTR are introduced.

Ibrahim et al. [7] studied numerically the impact of the wire coil on a PTC's overall performance. Their results show that the triangular wire coil inserts enhance the mixing of fluids inside the receiver resulting a decrease of the tube circumferential temperature. Reddy et al. [8] presented an experimental study of a rotary receiver in PTC technology. They reported that a rotary receiver improves the overall PTC's thermal comparing with stationary tube.

Elumalai et al. [9] investigated experimentally a modified PTC's absorber tube. Their results show that the modified absorber gives better thermal efficiency compared with conventional tube, and also it increases the heat transfer inside the absorber. Wang et al. [10] introduced an asymmetric corrugated tube of PTC in order to improve the system's reliability and heat transfer. They concluded that the use of this tube can augment the system efficiency.

Zhen et al. [11] presented a numerical study of an enhanced receiver tubes of a PTC on fully developed mixed turbulent. They demonstrated that dimpled absorber tubes operate better under nonuniform heat flux than they do under uniform heat flux and that increased heat transfer is achieved by flow reattachment, impingement, and vortex generation.

Bellos et al. [12] studied a diverging and converging receiver of PTC using nanofluids. According to their findings, the absorber tube with a wavy inner geometry leads to generate turbulent in the flow and improve the thermal efficiency compared to usual tube geometry. Also, the use of Al₂O₃ nanoparticles inside the HTF increases the average efficiency of the system. In another work [13] the same authors presented the impact of the introduction of internal longitudinal fins into an absorber tube of parabolic trough solar collectors. According to their result, the highest longitudinal fins lead to better thermal performance and at the same time higher pressure drop. They also show that the helium can be considered the best working fluid according to exergetic analysis compared to air and CO₂. Huang et al. [14] analyzed the thermal performance of a PTC absorber tube using dimpled surface, protrusions fins, and helical fins. Their results show that the deeper dimples,

small pitches and as much as inserts improve the thermal behavior of the tube.

Aggrey et al. [15] investigated numerically the thermodynamic performance of a PTC's receiver using perforated inserts placed centralized into the tube. They reported that the inserts enhance the system thermal efficiency, and also decrease the receiver temperature difference. Besides, The addition of the fins to the receiver improves the thermal performance and minimizes the entropy generation. In another work presented by the same authors [16], they investigated numerically a wall twisted inserts receiver tube. They concluded that as the twist ratio decreases, both the heat transfer and fluid friction factor augment, and as the width ratio increases, the heat transfer performance increases. And also, the use of twisted inserts decreases the receiver temperature difference.

Diwan and Soni. [17] presented an analysis of the PTC receiver tube thermal behavior using coils inserts. They concluded that better thermal performance is obtained in the case lower flowrates and 6 mm to 8 mm inserts pitch and at higher flow rates. Xingwang et al. [18] studied numerically a PTC's absorber tube under nonuniform heat flux distribution using helical screw-tape inserts. Various parameters that affect the thermal behavior of system are investigated, the impact of the solar incidence angle, the absorber tube heat losses, the maximum temperature and the outer surface of the absorber tube temperature gradient.

Cheng et al. [19] Investigated heat transfer improvement by using unilateral fins on absorber tubes in parabolic trough solar collectors. They concluded the unilateral fins give better heat transfer than that of the plain tube under the same operating conditions.

Ghadirijafarbigloo et al. [20] presented a numerical study of the thermal performance in a PTC's absorber tube using twisted-tape fins. Their results show that the introduction of twisted-tape inserts leads to high *Nu* number with a penalty of pressure drop compared with smooth tube. Reddy et al. [21] introduced different type of inserts in a tube receiver of a PTC. They observed that the trapezoidal porous fins enhance the heat transfer, and also, the heat losses by natural convection decrease by introducing trapezoidal fins compared with smooth tube. Another work presented by Reddy and Satyanarayana. [22] in which they proposed a numerical investigation of energy efficiency of a PTC receiver to show the thermal behavior of the receiver tube. According to their findings, the porous inserts cause a pressure drop while increasing the absorber tube thermal performance. Also, they reported that the heat transfer was increased due to the increase of the thermal conductivity, heat transfer area, and turbulence. In this paper a numerical investigation carried out to evaluate the heat transfer performance of PTC receiver tube and show the impact of the transversal fins placed on the focal region of the receiver tube on the thermos-hydraulic performance of the absorber tube using FVM coupled MCRT method.

2. PHYSICAL MODEL

Figure 1 shows a typical parabolic trough collector, it consists of a concentrator which is a parabolic mirror, and a receiver running along its focal line. This technology gives concentration only in one dimension. On the other

hand, the one-dimensional arrangement is mechanically simpler. The axis is aligned north-south, and the structure rotates automatically about its axis to follow the sun. The concentrator is a large parabolic shaped surface painted with reflective material in order to reflect the maximum solar radiation along its focal line. Besides, the receiver tube is the primordial element of this technology, where the solar rays are concentrated and transformed to usable energy form. The absorber tube is a stainless-steel tube selectively coated. To reach high efficiency, its emissivity should be small in the IR wavelength range and its absorption should be higher in the visible light wavelength. A glass tube that has a high transmissivity envelope the absorber tube. The gap between those two tubes (annular space) is maintained under vacuum ($P < 0.013Pa$) with the objective to minimize the heat losses by convection [23]. The characteristics of the PTC solar concentrator are presented in table 1.

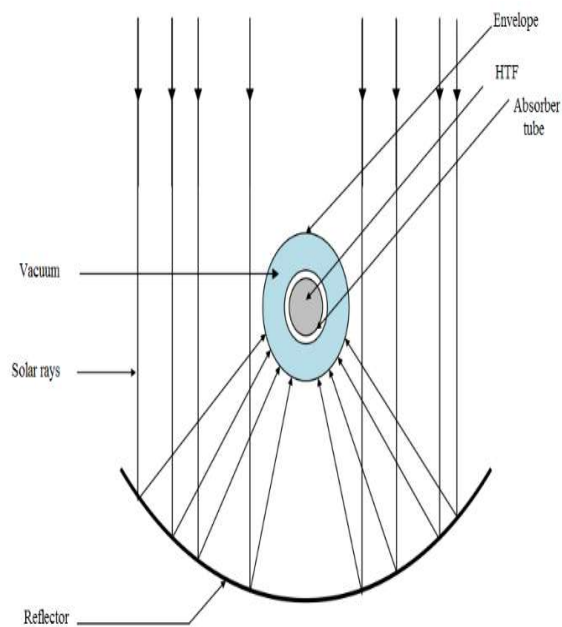


Fig. 1. Parabolic Trough Collector sketch

Table 1. Characteristics of the PTC solar concentrator [24]

| | |
|------------------------------|--------------------|
| Focal length | 1.71 m |
| Reflector aperture | 5.77 m |
| Envelope Material | Borosilicate glass |
| Envelope transmittance | 96% |
| Glass cover internal radius | 5.95 cm |
| Glass cover external radius | 6.25 cm |
| Inner radius of the absorber | 95% |
| Outer radius of the absorber | 3.2 cm |
| Coating absorbance | 3.5 cm |

As shown in figure 2, the solar rays are focused on the bottom outer wall of the receiver, while non-concentrated sun rays strike the topper part. Transversal fin inserts are added to the absorber tube's bottom part in the aim of improving the receiver tube thermal efficiency and reduce the receiver circumferential temperature gradient, and also minimize the heat losses, transversal fin inserts are introduced into the absorber tube and inserted on the inner surface of the receiver as shown in figure 2.

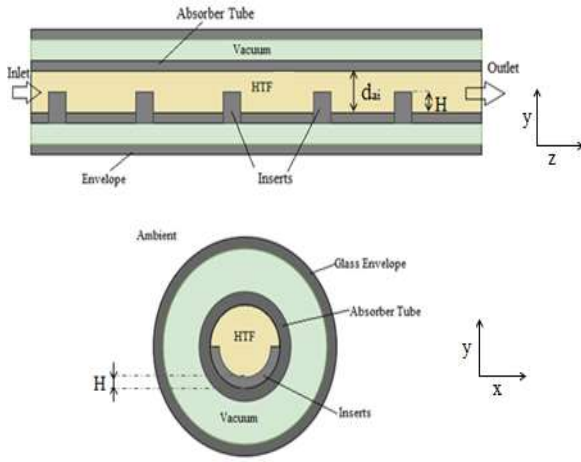


Fig. 2. Sketch of the enhanced tube

3. MATHEMATICAL MODEL

a. Governing equations:

The computational fluid dynamics governing equations are [25]:

- **Continuity equation:**

$$\frac{\partial}{\partial x_j}(\rho u_i) = 0 \quad (1)$$

- **Momentum equation:**

$$\begin{aligned} \frac{\partial}{\partial x_i}(\rho u_i u_j) = & -\frac{\partial P}{\partial x_i} \\ & + \frac{\partial}{\partial x_j} \left[(\mu + \mu_t) \left(\frac{\partial u_i}{\partial x_j} + \frac{\partial u_j}{\partial x_i} \right) \right. \\ & \left. - \frac{2}{3} (\mu + \mu_t) \frac{\partial u_i}{\partial x_i} \delta_{ij} \right] + \rho g_i \end{aligned} \quad (2)$$

- **Energy equation:**

$$\frac{\partial}{\partial x_i}(\rho u_i T) = \frac{\partial}{\partial x_i} \left[\left(\frac{\mu}{Pr} + \frac{\mu_t}{\sigma_t} \right) \frac{\partial T}{\partial x_i} \right] \quad (3)$$

There are two model equations in the standard k - ε equations [25]:

- **k -equation:**

$$\frac{\partial}{\partial x_i}(\rho u_i k) = \frac{\partial}{\partial x_i} \left[\left(\mu + \frac{\mu_t}{\sigma_k} \right) \frac{\partial k}{\partial x_i} \right] + G_k - \rho \varepsilon \quad (4)$$

- **ε -equation:**

$$\begin{aligned} \frac{\partial}{\partial x_i}(\rho u_i \varepsilon) = & \frac{\partial}{\partial x_i} \left[\left(\mu + \frac{\mu_t}{\sigma_\varepsilon} \right) \frac{\partial \varepsilon}{\partial x_i} \right] \\ & + \frac{\varepsilon}{k} (c_{1\varepsilon} G_k - c_{2\varepsilon} \rho \varepsilon) \end{aligned} \quad (5)$$

Where G_k represent the turbulent kinetic energy generation:

$$G_k = \mu_t \frac{\partial u_i}{\partial x_i} \left(\frac{\partial u_i}{\partial x_j} + \frac{\partial u_j}{\partial x_i} \right) + \frac{2}{3} \rho k \delta_{ij} \frac{\partial u_i}{\partial x_j} \quad (6)$$

μ_t is the turbulent viscosity and it is defined as:

$$\mu_t = C_\mu \rho \frac{k^2}{\varepsilon} \quad (7)$$

The turbulence equations have five constants C_μ , σ_k , σ_ε , $c_{1\varepsilon}$ and $c_{2\varepsilon}$ [26]:

$$C_\mu = 0.09, \sigma_k = 1.00, \sigma_\varepsilon = 1.30,$$

$$c_{1\varepsilon} = 1.44 \text{ and } c_{2\varepsilon} = 1.92$$

b. Boundary conditions:

- **Inlet fluid condition:**

$$\begin{aligned} V_x &= V_{in} \\ V_y &= V_z = 0 \\ T_f &= T_{in} \end{aligned}$$

- **Outlet fluid conditions:**
- **Fully developed turbulent flow.**
- **No-slip conditions on the inner surface of the receiver.**
- **Nonuniform heat flux distribution on the absorber tube's outside wall (fig. 4) [27]:**

$$q = LCR \cdot DNI \quad (8)$$

Where the DNI is the Direct normal irradiation ($DNI = 1000 \text{ W} \cdot \text{m}^{-2}$)

- The glass cover outer wall is considered under mixed boundary condition.

The temperature of the sky is defined as [27]:

$$T_{sky} = 0.00552 \cdot T_{amb}^{1.5} \quad (9)$$

Where T_{amb} is ambient temperature.

The convective coefficient of the wind is expressed as [28]:

$$h_w = 4 \cdot V_w^{0.58} \cdot d_{go}^{-0.48} \quad (10)$$

V_w is the wind velocity, ($V_w = 2.5 \text{ m} \cdot \text{s}^{-1}$) and d_{go} is the glass pipe outer diameter.

The MCRT approach was employed in this investigation to display the distribution of the solar heat flux on the receiver's outer wall [26].

The governing equations are discretized and solved using FVM method.

Figure 3 presents the LCR in function of the of the absorber tube circumferential angle. As can be observed, there is a nonuniform heat flux distribution over the absorber tube's outer surface, which results in a nonuniform distribution of temperature.

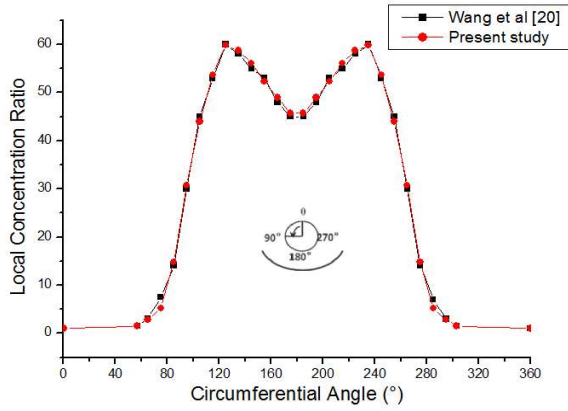


Fig. 3. Local Concentration Ration in function of the absorber tube circumferential angle [26].

a. Thermo-physical properties of HTF:

Therminol®VP1 is used as HTF in this investigation, [29]. The thermo-physical properties of the HTF liquid phase as a function of temperature are taken from [24].

4. MODEL VALIDATION

With the aim to show the numerical model accuracy, the results of the numerical simulation and the results calculated from the literature correlations are compared.

The average *Nu* number is expressed as:

$$Nu = \frac{hd_{ai}}{\lambda} \tag{11}$$

And

$$h = \frac{Q}{T_{ai} - T_f} \tag{12}$$

Where *Q*, *T_f* and *T_{ai}* are the mean heat flux, the bulk average temperature, and the absorber tube inner surface average temperature.

The Darcy friction factor *f* under turbulent flow conditions in plain circular tube is expressed as:

$$f = \frac{2d_{ai}\Delta P}{L\rho u^2} \tag{13}$$

Where *d_{ai}* is the internal tube diameter, and *L* is the tube length.

The *Nu* number correlation of Gnielinski [32] is given by:

$$Nu = \frac{\frac{f}{8}(Re - 1000)Pr}{1 + 12.7\left(\frac{f}{8}\right)^{0.5}\left(Pr^{\frac{2}{3}} - 1\right)} \tag{14}$$

The Petukhov correlation [30, 31] under turbulent flow conditions in plain circular tube is used to calculate the friction factor *f*.

$$f = (0.79 \ln Re - 1.64)^{-2} \begin{cases} 0.5 \leq Pr \leq 2000 \\ 3000 \leq Re \leq 5 \cdot 10^6 \end{cases} \tag{15}$$

Another equation to determine the average Nusselt number presented by Notter [32] and it is expressed as:

$$Nu = 5 + 0.015 Re^{0.856} \cdot Pr^{0.347} \tag{16}$$

Also, another correlation of Darcy friction factor *f* calculation for established internal flow in plain pipes is proposed by Blasius [32] and it is expressed as:

$$f = 0.184 Re^{-0.2} \quad (Re \geq 2 \cdot 10^4) \tag{17}$$

Figure 4. presents the evolution of the *Nu* in function of *Re* for both numerical results and results calculated using numerical correlations respectively. As shown, the *Nu* evolution in function of the *Re* agree well with each other accompanied with a maximum error of 2.65 % and 4.43 % for Gnielinski and Notter curves respectively.

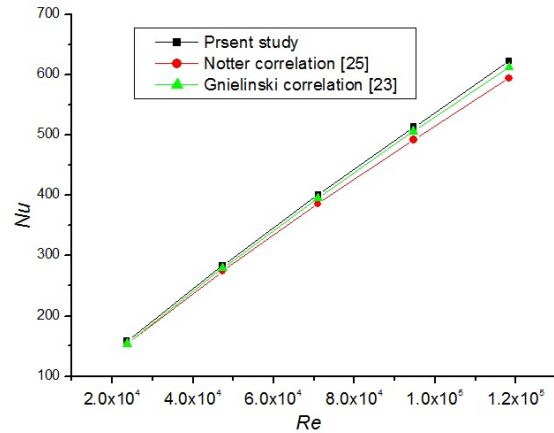


Fig. 4. evolution of *Nu* number in function of *Re* number for smooth tube

Figure 5 shows the curves of the Darcy friction factor *f* obtained numerically and the friction factor calculated by correlation of Petukhov and Blasius with the maximum error of 4.86 % and 6 % respectively. From this it can be considered that the numerical model can be used for further investigation.

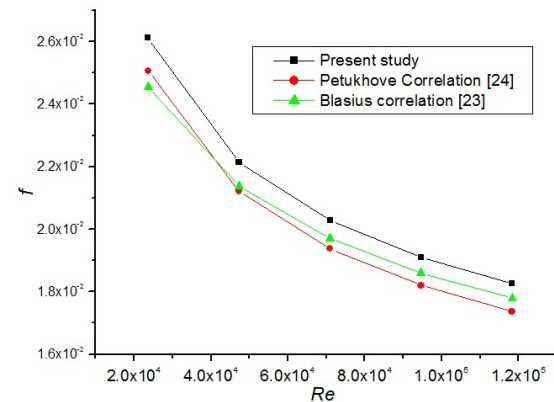


Fig. 5. evolution of *f* number in function of *Re* number for smooth tube.

5. RESULTS AND DISCUSSION

The effect of the fin's height on the thermal performance of the enhanced tube is demonstrated in this section. For this purpose, five different inserts of different heights are introduced into the absorber tube $H/d_{ai} = 0.078, 0.109, 0.14$ and 0.171 .

The evolution of the Nu number in function of the Re number is presented in Figure 6. This figure demonstrates that, for both smooth and improved tube, as the Re number rises, the Nu number rises as well, and that, at a given Re number, as the height of the inserts (H/d_{ai}) increases, the Nu number increased also. Additionally, it can be demonstrated that the enhanced tube's Nu number is higher than the conventional tube in all insert's height cases.

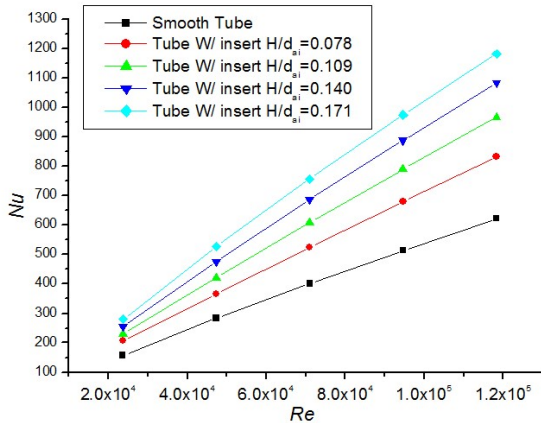


Fig. 6. evolution of Nu in function of Re for different H/d_{ai} values

The evolution of the Darcy friction factor f in function of insert heights and Re number is depicted in Figure 7. For a given Re number, the friction factor f augments with the augment of the insert height, but it also decreases with the augment in the Re . This is due to the increase in the pressure brought on by the generation of vortices and the dissipation of turbulence energy inside the tube.

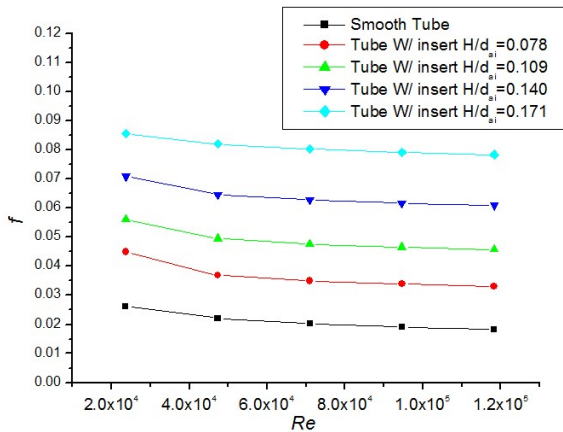


Fig. 7. evolution of f in function of Re for different H/d_{ai} values

With the objective of evaluating the thermohydraulic performance of the proposed technic with respect the

conventional one, it is assessed using the Performance Evaluation Criteria (PEC), and it is expressed as [33]:

$$PEC = \frac{(Nu/Nu_s)}{(f/f_s)} \tag{18}$$

Figure 8 shows PEC evolution for various insert heights in function of Re number. This figure demonstrates that the PEC of the suggested tubes is consistently greater than 1, and the best thermal performance is provided by the tube with the highest inserts ($H/d_{ai} = 0.171$).

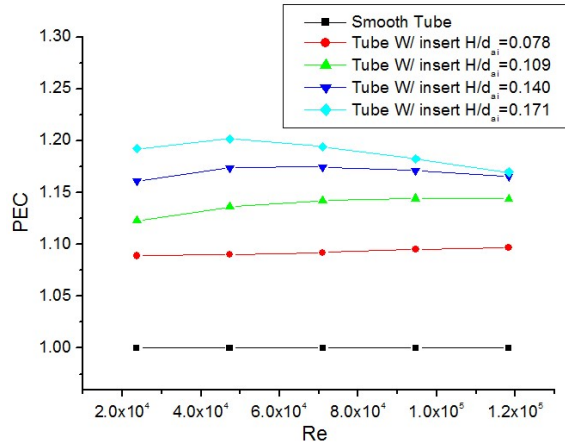


Fig. 8. Evolution of the PEC in function of Re for different H/d_{ai} values

The distribution of the temperature in function of the circumferential angle of the receiver outer wall for both smooth and enhanced tube is presented in figure 9. It is shown that the tube wall temperature distribution is nonuniform because of the nonuniformity of the heat flux over the receiver. It can be concluded that the fins help to reduce heat losses to the environment and uniformize the temperature of the tube's wall by utilizing this sort of fins within the smooth tube. Also, it is observed that the gradient of the temperature reduces as the insert's height increases.

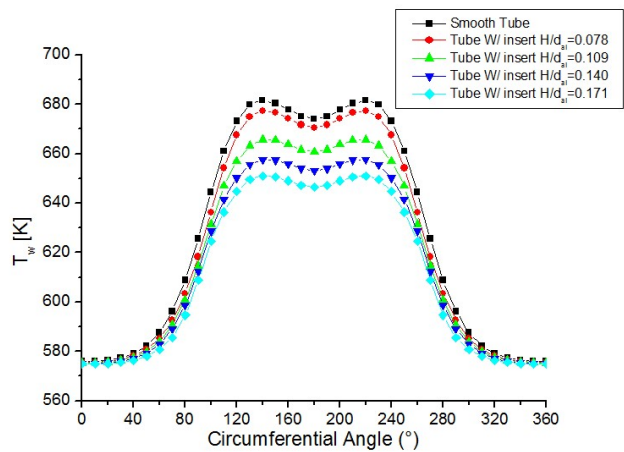


Fig. 9. Circumferential temperature distribution over the tube for different dimensionless inserts height H/d_{ai}

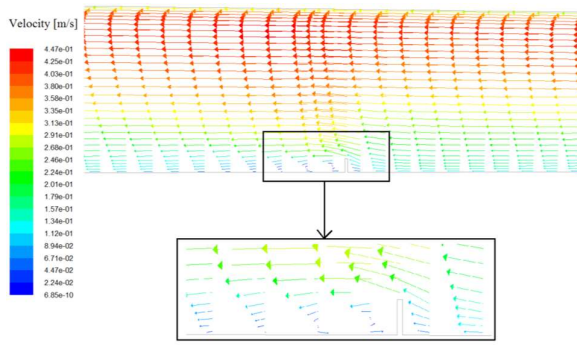
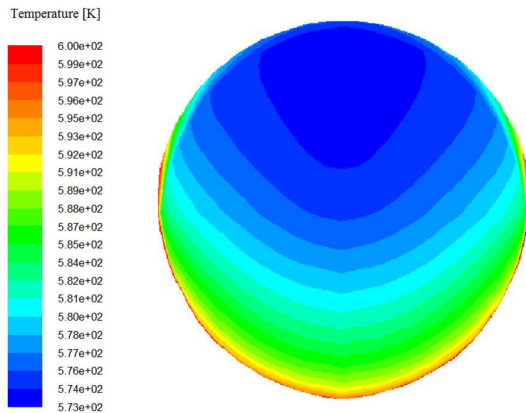


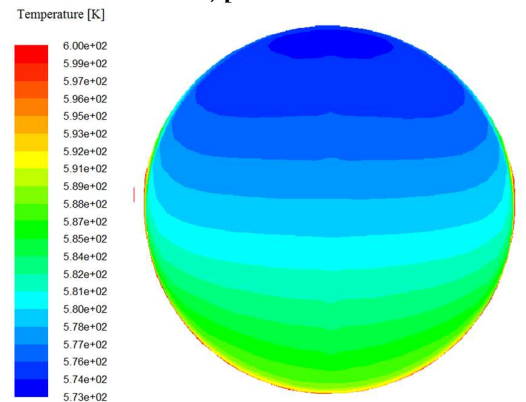
Fig. 10. Velocity vector distribution of the enhanced tube in the case of ($H/d_{ai} = 0.171$ and $Re = 70.979 \cdot 10^3$).

Figure 10 shows the velocity vector of the HTF inside the tube in the case of height inserts ($H/d_{ai} = 0.171$) and $Re = 70.979 \cdot 10^3$. As shown in this figure the introduction of fins inside the smooth tube, the HTF's field velocity increases with respect to the plain tube, and it help to generate vortices which leads to increases the turbulence and homogenize the HTF temperature.

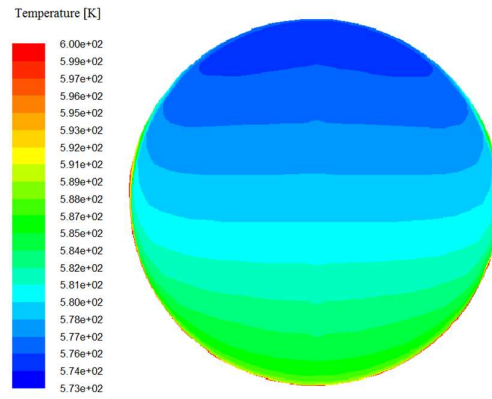
Figure 11 presents *HTF* temperature contour of the plain tube and the improved tube at the exist for all cases of inserts height (H/d_{ai}) and at $Re = 70.979 \cdot 10^3$. As shown, the *HTF* temperature distribution at the tube outlet can be homogenized by introducing the inserts with respect to the plain tube, and also, the HTF bulk temperature at the receiver exist augments as the dimensionless insert's height (H/d_{ai}) increases.



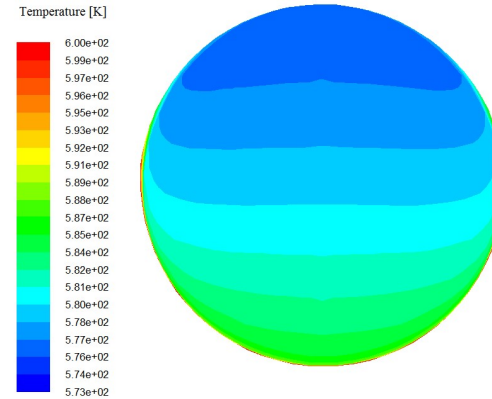
a) plain Tube



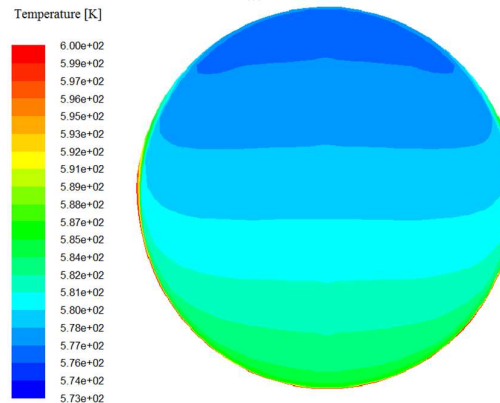
b) $H/d_{ai} = 0.078$



c) $H/d_{ai} = 0.109$



d) $H/d_{ai} = 0.140$



e) $H/d_{ai} = 0.171$

Fig. 11. HTF temperature contour at the exist of the tube

6. CONCLUSION

In this study we analyzed the impact of the introduction of the inserts on the bottom periphery of the absorber tube. The height of the inserts is optimized to increase the thermal performance of the system. The numerical results lead to the following conclusions under the conditions studied:

- 1) The temperature of receiver outer surface is nonuniform due to the heat flux nonuniformity distribution on the receiver outer wall.
- 2) As compared to the conventional PTC receiver, the inserts raise the Nu number to 1.9 times and the Darcy friction factor to 4.29 times.

- 3) The Performance Evaluation Criteria (PEC) proves that the use of the inserts gives always good heat transfer enhancement inside the receiver.
- 4) The use of the inserts on the bottom part of the receiver decreases the circumferential temperature gradient of the absorber tube.
- 5) The height and the width of the inserts have remarkable influence on the thermal performance of the absorber tube.

Nomenclature

| | |
|---------|---|
| C_p | Specific heat capacity, $J \cdot kg^{-1} \cdot K^{-1}$ |
| d | Diameter, m |
| f | Friction factor |
| g | Gravitational acceleration, $m \cdot s^{-2}$ |
| h | Convection heat transfer coefficient, $W \cdot m^{-2} \cdot K^{-1}$ |
| H | Height of inserts, m |
| L | Length, m |
| Nu | Nusselt number |
| P | Pressure, Pa |
| Q | Heat flux, $W \cdot m^{-2}$ |
| Re | Reynolds number |
| T | Temperature, K |
| u | Velocity component, $m \cdot s^{-1}$ |
| V | Velocity magnitude, $m \cdot s^{-1}$ |
| x,y,z | Cartesian coordinate, m |

Greek

| | |
|---------------|---|
| ρ | Density, $kg \cdot m^{-3}$ |
| λ | Thermal conductivity, $W \cdot m^{-1} \cdot K^{-1}$ |
| μ | Dynamic viscosity, $N \cdot m^{-2} \cdot s^{-1}$ |
| μ_t | Turbulent viscosity, $N \cdot m^{-2} \cdot s^{-1}$ |
| ν | Kinematic viscosity, $m^2 \cdot s^{-1}$ |
| k | Turbulent kinetic energy, $m^2 \cdot s^{-2}$ |
| ε | Turbulent dissipation rate, $m^2 \cdot s^{-3}$ |
| G_k | generation of turbulence kinetic energy |

Subscribe

| | |
|----|------------------------|
| ai | Absorber inner wall |
| f | Fluid |
| go | Glass cover outer wall |
| s | Smooth tube |
| w | Wind |

Abbreviation

| | |
|------|---------------------------------|
| DNI | Direct Normal Irradiance |
| FVM | Finite Volume Method |
| HTF | Heat Transfer Fluid |
| LCR | Local Concentration Ratio |
| MCRT | Monte Carlo Ray Trace |
| PEC | Performance Evaluation Criteria |
| PTC | Parabolic Trough Collector |

REFERENCES

- [1]. Ari R.: Active solar collectors and their applications, Center for Energy and Environmental Studies, Princeton University, Oxford university press, 1985.
- [2]. Kai Z., Hongguang J., Zhongrui G., and Hui H. A thermal efficiency-enhancing strategy of parabolic trough collector systems by cascadingly applying multiple solar selective-absorbing coatings. Applied Energy, 309, (2022), 118508.
- [3]. Natraj and K.S. Reddy. Investigations of thermo-structural instability on the performance of solar parabolic trough

- collectors. Renewable Energy, 202, (2023), 381–393.
- [4]. Ratzel A. C. Hickox C. E. and Gartling D. K.: Techniques for reducing thermal conduction and natural convection heat losses in annular receiver geometries, Journal of Heat Transfer, 101, (1979),108-113.
- [5]. Haddouche M. R and Benazza A. Numerical investigation and solar flux distribution analysis of parabolic trough solar collector by adding secondary reflector. Instrumentation Mesure Métrologie, 18, (2019), 275-280.
- [6]. Gong X., Wang F., Wang H., Tan J., Lai Q. and Han H.: Heat transfer enhancement analysis of tube receiver for parabolic trough solar collector with pin fin arrays inserting, Solar Energy, 144, (2017), 185–202.
- [7]. İbrahim H. Y., Aggrey M., and Taha T. G. Enhancing the overall thermal performance of a large aperture parabolic trough solar collector using wire coil inserts. Sustainable Energy Technologies and Assessments, 39, (2020), 100696
- [8]. N. S. Reddy, S. G. Subramanya, K.C. Vishwanath, M. Karthikeyan, and S. Kanchiraya. Enhancing the thermal efficiency of parabolic trough collector using rotary receiver tube. Sustainable Energy Technologies and Assessments, 51, (2022), 101941.
- [9]. Elumalai V., Abdul Rahim I. R., Rohan M., Sattwik H., and Ramalingam S. Heat transfer enhancement of a parabolic trough solar collector using a semicircular multitube absorber. Renewable Energy, 196, (2022), 111-124.
- [10]. Wang F., Tang Z., Gong X., Tan J., Han H. and Li B.: Heat transfer performance enhancement and thermal strain restrain of tube receiver for parabolic trough solar collector by using asymmetric outward convex corrugated tube, Energy, 114, (2016), 275-292.
- [11]. Zhen H., Zeng-Yao L., Guang-Lei Y. and Wen-Quan T.: Numerical investigations on fully developed mixed turbulent convection in dimpled parabolic trough receiver tubes, Appl. Therm. Eng, (2016).
- [12]. Bellos E., Tzivanidis C., Antonopoulos K. A., and Gkinis G.: Thermal enhancement of solar parabolic trough collectors by using nanofluids and converging-diverging absorber tube, Renewable Energy, 94, (2016), 213-222.
- [13]. Bellos E., Tzivanidis C., Antonopoulos K. A., and Daniil I.: The impact of internal longitudinal fins in parabolic trough collectors operating with gases, Energy Conversion and Management, (2017), 135, 35–54.
- [14]. Huang Z., Yua G.L., Li Z.Y. and Tao W.Q.: Numerical study on heat transfer enhancement in a receiver tube of parabolic trough solar collector with dimples, protrusions and helical fins, Energy Procedia, 69, (2015), 1306 – 1316.
- [15]. Aggrey M., Tunde B. O. and Josua P. M.: Heat transfer and thermodynamic performance of a parabolic trough receiver with centrally placed perforated plate inserts, Appl. Energy, (2014).
- [16]. Aggrey M., Tunde B. O. and Josua P. M.: Heat transfer and entropy generation in a parabolic trough receiver with wall-detached twisted tape inserts, International Journal of Thermal Sciences, 99, (2016), 238-257.
- [17]. Ketan D. and Soni M.S.: Heat Transfer Enhancement in absorber tube of parabolic trough concentrators using wire-coils inserts, UJME, 3, (2015), 107-112.
- [18]. Xingwang S., Guobo D., Fangyuan G., Xungang D., Liqing Z., and Fuyun Z.: A numerical study of parabolic trough receiver with nonuniform heat flux and helical screw-tape inserts, Energy, (2014), 1-12.
- [19]. Cheng Z.D., He Y.L. and Cui F.Q.: Numerical study of heat transfer enhancement by unilateral longitudinal vortex generators inside parabolic trough solar receivers, International Journal of Heat and Mass Transfer, 55, (2012), 5631–5641.
- [20]. Ghadirijafarbeigloo Sh., Zamzambianb A. H. and Yaghoubic M.: 3-D numerical simulation of heat transfer and turbulent flow in a receiver tube of solar parabolic

- trough concentrator with louvered twisted-tape inserts, *Energy Procedia*, 49, (2014), 373 – 380.
- [21]. Reddy K. S. and Satyanarayana G. V.: Numerical study of porous finned receiver for solar parabolic trough concentrator, *Engineering Applications of Computational Fluid Mechanics*, 2, (2008), 172–184.
- [22]. Reddy K. S., Ravi K. K. and Satyanarayana G. V.: Numerical Investigation of Energy-Efficient Receiver for Solar Parabolic Trough Concentrator, *Heat Transfer Engineering*, 29, (2011), 961-972.
- [23]. Yanjuan W., Qibin L., Jing L. and Hongguang J. : A three-dimensional simulation of a parabolic trough solar collector system using molten salt as heat transfer fluid, *Applied Thermal Engineering*, 70, (2014), 462-476.
- [24]. Chun C., Adriano S., Zhiyong W., Xin L., Yongliang L., Mingzhi Z., Jie D., Zhifeng W., and Yulong D.: Enhanced heat transfer in a parabolic trough solar receiver by inserting rods and using molten salt as heat transfer fluid, *Applied Energy*, 220(2018), 337–350.
- [25]. Launder B.E. and Spalding G D.B.: The numerical computation of turbulent flows, *COMPUTER METHODS IN APPLIED MECHANICS AND ENGINEERING*, 3, (1974), 269-289.
- [26]. Versteeg H.K. and Malalasekera W.: An introduction to computational fluid dynamics, the finite volume method, John Wiley and Sons Ink, New York, 1995.
- [27]. Swinbank W. C.: Long-wave radiation from clear skies, Division of Meteorological Physics, Aspendale, Australia, (1963), 339-348.
- [28]. Mullick S. C. and Nanda S. K.: An improved technique for computing the heat loss factor of a tubular absorber, *Solar Energy*. 42, (1989), 1-7.
- [29]. Heat transfer fluids by SOLUTIA, Applied chemistry, creative solutions.
- [30]. Yunus A. C.: Heat and mass transfer A PRACTICAL APPROACH, MC Graw Hill, Third ed, 2007.
- [31]. Petukhov. B. S.: Heat transfer and friction in turbulent pipe flow with variable physical properties, High Temperature Institute. Academy of Science of the USSR. Moscow, (1970), 504-561.
- [32]. Notter R. H. and Sleicher C. A.: A solution to the turbulent Graetz problem-III Fully developed and entry region heat transfer rates, *Chemical Engineering Science*, 27, (1972), 2073-2093.
- [33]. Khwanchit W. and Smith E.: Enhancement of heat transfer using CuO/water nanofluid and twisted tape with alternate axis, *International Communications in Heat and Mass Transfer*, 38, (2011), 742–748.